Development 135, 1481-1491 (2008) doi:10.1242/dev.020255

Direct interaction of *AGL24* and *SOC1* integrates flowering signals in *Arabidopsis*

Chang Liu[1,2], Hongyan Chen[1,2], Hong Ling Er[1], Hui Meng Soo[3], Prakash P. Kumar[1,2], Jin-Hua Han[1], Yih Cherng Liou[1] and Hao Yu[1,2,*]

During the transition from vegetative to reproductive growth, the shoot meristem of flowering plants acquires the inflorescence identity to generate flowers rather than vegetative tissues. An important regulator that promotes the inflorescence identity in *Arabidopsis* is AGAMOUS-LIKE 24 (AGL24), a MADS-box transcription factor. Using a functional estradiol-inducible system in combination with microarray analysis, we identified *AGL24*-induced genes, including *SUPPRESSOR OF OVEREXPRESSION OF CO 1* (*SOC1*), a floral pathway integrator. Chromatin immunoprecipitation (ChIP) analysis of a functional *AGL24-6HA*-tagged line revealed in vivo binding of AGL24-6HA to the regulatory region of *SOC1*. Mutagenesis of the AGL24 binding site in the *SOC1* promoter decreased Pro_{SOC1}*:GUS* expression and compromised *SOC1* function in promoting flowering. Our results show that *SOC1* is one of the direct targets of *AGL24*, and that *SOC1* expression is upregulated by *AGL24* at the shoot apex at the floral transitional stage. ChIP assay using a functional *SOC1-9myc*-tagged line and promoter mutagenesis analysis also revealed in vivo binding of SOC1-9myc to the regulatory regions of *AGL24* and upregulation of *AGL24* at the shoot apex by *SOC1*. Furthermore, we found that as in other flowering genetic pathways, the effect of gibberellins on flowering under short-day conditions was mediated by the interaction between *AGL24* and *SOC1*. These observations suggest that during floral transition, a positive-feedback loop conferred by direct transcriptional regulation between *AGL24* and *SOC1* at the shoot apex integrates flowering signals.

KEY WORDS: Flowering time, MADS-box transcription factor, Transcriptional regulation, Chromatin immunoprecipitation, Gibberellin, *Arabidopsis*

INTRODUCTION

The transition from vegetative to reproductive development in *Arabidopsis* is mediated by multiple genetic pathways in response to developmental cues and environmental signals (Amasino, 2004; Balasubramanian et al., 2006; Blazquez et al., 2003; Cerdan and Chory, 2003; Halliday et al., 2003; Simpson and Dean, 2002). The photoperiod pathway perceives the light quantity and circadian clock, whereas the vernalization pathway responds to low temperatures. The autonomous pathway monitors endogenous cues from specific developmental states, which are independent of environmental signals. The gibberellin (GA) pathway particularly regulates flowering in non-inductive short-day conditions. In addition to these major genetic pathways, the pathways mediating the responses to various wavelengths of light and temperature alteration above a critical threshold have also been suggested to affect flowering. An intricate network of the above pathways promotes floral transition via transcriptional regulation of several floral pathway integrators including *FLOWERING LOCUS T* (*FT*), *SUPPRESSOR OF OVEREXPRESSION OF CO 1* (*SOC1*; also known as *AGL20* – TAIR) and *LEAFY* (*LFY*) (Boss et al., 2004; Mouradov et al., 2002; Parcy, 2005; Simpson and Dean, 2002).

MADS-box genes encode a large family of transcription factors in plants that share a highly conserved MADS-box domain, which recognizes the $CC(A/T)_6GG$ (CArG) box on target genes for binding (Riechmann et al., 1996; Shore and Sharrocks, 1995). In *Arabidopsis*, the MADS-box gene family is a major class of regulators mediating floral transition. *AGAMOUS-LIKE 24* (*AGL24*) is one of the MADS-box genes found to promote flowering (Michaels et al., 2003; Yu et al., 2002). *AGL24* expression is detectable in the vegetative shoot apex and is upregulated in the inflorescence apex during floral transition. Transgenic studies of *35S:AGL24* and *AGL24* RNA interference lines have shown that the upregulated level of *AGL24* expression corresponds to the degree of precocious flowering and that the reduction in *AGL24* expression is related to the degree of late flowering, suggesting that *AGL24* is a dosage-dependent promoter of flowering.

The expression of *AGL24* is barely detectable in the center of emerging floral meristems and is present in floral reproductive organs at later stages (Yu et al., 2004). Overexpression of *AGL24* promotes flowering and transforms floral meristems into inflorescence meristems, indicating that *AGL24* specifically promotes inflorescence identity. Direct repression of *AGL24* and two other flowering time genes, *SOC1* and *SHORT VEGETATIVE PHASE* (*SVP*), by the floral meristem identity gene *APETALA1* (*AP1*), prevents the continuation of the shoot developmental program, contributing to the specification of floral meristem identity (Liu et al., 2007; Yu et al., 2004). On the other hand, expression of *AGL24* and *SVP* at an appropriate level in the floral meristem is also required for regulation of class B and C floral homeotic genes at a high temperature (Gregis et al., 2006). Therefore, *AGL24* regulates both flowering time and flower development.

Previous studies on the role of *AGL24* in flowering time control have revealed that *AGL24* and *SOC1* affect expression of each other (Michaels et al., 2003; Yu et al., 2002), implying that these two MADS-box transcription factors might directly or indirectly interact to mediate flowering. However, *AGL24* and *SOC1* are differently regulated during floral transition in several aspects. First, although *AGL24* expression is regulated by vernalization, it is independent of

[1]Department of Biological Sciences, Faculty of Science, National University of Singapore, Singapore 117543, Singapore. [2]Temasek Life Sciences Laboratory, 1 Research Link, National University of Singapore, Singapore 117604, Singapore. [3]Institute of Molecular and Cell Biology, Proteos, Singapore 138673, Singapore.

*Author for correspondence (e-mail: dbsyuhao@nus.edu.sg)

Accepted 22 February 2008

FLOWERING LOCUS C (*FLC*), a potent repressor of flowering (Michaels et al., 2003). By contrast, *FLC* represses *SOC1* expression in the meristem and also delays *SOC1* expression by repressing *FT*, which encodes a protein acting as a long-distance floral signal moving from the leaf to the meristem (Corbesier et al., 2007; Hepworth et al., 2002; Searle et al., 2006). Second, in the photoperiod pathway, *AGL24* is affected by *CONSTANS* (*CO*), but not by *FT* (Yu et al., 2002), whereas *SOC1* is mainly regulated by *FT* and indirectly by *CO* via an unknown DNA-binding factor (Hepworth et al., 2002; Lee et al., 2000; Samach et al., 2000). Lastly, alteration of *AGL24* activity determines flowering time partially independently of *SOC1*, and vice versa, indicating that they can promote flowering in independent pathways (Michaels et al., 2003; Yu et al., 2002). These observations suggest that *AGL24* perceives flowering signals that are different from those integrated by *SOC1*. Therefore, what the exact relationship is between *AGL24* and *SOC1* and how they interact to affect flowering are essential questions for understanding the integration of flowering signals.

In this study we established and applied a functional estradiol-inducible *AGL24* system in combination with microarray analysis to identify *AGL24*-induced genes including *SOC1*. We provide evidence that *AGL24* and *SOC1* directly regulate mutual transcription to integrate flowering signals from several genetic pathways, including the GA pathway. This direct interaction confers a positive-feedback regulation of the expression of *AGL24* and *SOC1* to a quantitative threshold required for the transition from vegetative to reproductive growth.

MATERIALS AND METHODS

Plant materials and growth conditions

Wild-type and transgenic *Arabidopsis* plants of the same Columbia ecotype were grown at 22°C under long-day (16 hours light/8 hours dark) or short-day (8 hours light/16 hours dark) conditions. GA treatment of plants was started with seedlings at 1 week after germination, and weekly application of 100 μM GA_3 was performed as published (Moon et al., 2003).

Plasmid construction and plant transformation

For the construction of pER22-*AGL24*, the *AGL24* cDNA was amplified with primers (restriction sites underlined) AGL24-F1-*Xho*I (5′-CCGCTCGAGGTAGTGTAAGGAGAGATCTGG-3′) and AGL24-R1-*Apa*I (5′-ATGGGCCCTTCCCAAGATGGAAGCCCAA-3′). The digested PCR products were cloned into the pER22 vector. The pER8 vector (Zuo et al., 2000) was cut with *Apa*I and *Spe*I, the cohesive ends filled in, and self-ligated to produce pER22.

To construct *35S:AGL24-6HA*, the *AGL24* cDNA was amplified with primers AGL24-F1-*Xho*I and AGL24-R1-*Apa*I. The digested PCR products were cloned into the pGreen-35S-6HA vector to obtain an in-frame fusion of *AGL24-6HA* under the control of the 35S promoter. The pGreen-35S-6HA vector was generated by cloning six repetitive HA epitopes into the *Spe*I site of pGreen-35S (Yu et al., 2004).

To construct *35S:SOC1-9myc*, the *SOC1* cDNA was amplified with primers SOC1-F1-*Xho*I (5′-CCGCTCGAGTAGCCAATCGGGAAATTAACTA-3′) and SOC1-R1-*Xma*I (5′-CGCCCGGGCTTTCTTGAAGAACAAGGTAAC-3′). The digested PCR products were cloned into the pGreen-35S-9myc vector to obtain an in-frame fusion of *SOC1-9myc* under the control of the 35S promoter. The pGreen-35S-9myc vector was generated by cloning nine repetitive myc epitopes into the *Spe*I site of pGreen-35S.

To construct Pro_{SOC1}*:GUS*, the 2.0 kb *SOC1* 5′ upstream sequence (Fig. 4C) was amplified with the primers SOC1-P4-*Xma*I (5′-AACCCGGGATCGTATTTACTAGTGGTATACG-3′) and SOC1-R2-*Xma*I (5′-AACCCGGGATCTTCTTCTTTAGTTAATTTCCC-3′). The digested PCR products were cloned into the pHY107 vector (Liu et al., 2007). This construct was mutagenized to produce the mutated AGL24 binding site (Fig. 4C) using the QuikChange II XL Site-Directed Mutagenesis Kit (Stratagene).

To construct Pro_{AGL24}*:GUS*, the 4.7 kb *AGL24* genomic sequence (Fig. 5F) was amplified with primers AGL24-P1-*Pst*I (5′-AACTGCAGTCGTTCCTTATAGCGGTGGAT-3′) and AGL24-P4-*Spe*I (5′-GGACTAGTTTCCCAAGATGGAAGCCTAACCAAC-3′). The digested PCR products were cloned into pHY107. This construct was mutagenized to produce the mutated sites of M-2003 and M-2039 (Fig. 5F).

For the complementation test, the *AGL24* genomic fragment was amplified with primers AGL24-P1-*Pst*I and AGL24-p-R-*Xba*I (5′-CCTCTAGATCATTCCCAAGATGGAAGCC-3′), and the *SOC1* genomic fragment was amplified with primers SOC1-P4-*Xma*I and SOC1-p-R-*Xba*I (5′-CCTCTAGATCACTTTCTTGAAGAACAAGG-3′). The digested PCR products were cloned into pHY105 (Liu et al., 2007). The constructs containing the mutated forms of the genomic *AGL24* and *SOC1* fragments were generated using the QuikChange II XL Site-Directed Mutagenesis Kit.

For the complementation test, the relevant constructs were introduced into *agl24-1* or *soc1-2*, whereas other constructs were introduced into wild-type Columbia plants using the *Agrobacterium*-mediated floral dip method (Clough and Bent, 1998). Except for transgenic plants with the pER22-*AGL24* construct that were selected on MS medium (Sigma) supplemented with hygromycin, transgenic plants with other constructs were selected by Basta.

β-estradiol induction of pER22-*AGL24*

To observe the phenotype of pER22-*AGL24* plants upon β-estradiol induction, they were grown on solid MS medium supplemented with 1% sucrose at 22°C under long-day conditions before applying various treatments. Once we started the treatment, 10 μM β-estradiol was applied and replaced every 2 days. For examining the induction of *AGL24* by estradiol, the seedlings at different developmental stages grown on solid MS medium were transferred into liquid MS medium supplemented with 10 μM β-estradiol. These seedlings were incubated in the liquid medium with gentle shaking for 1 to 24 hours. Mock treatment of transgenic plants was also performed for the above experiments in which the solvent dimethyl sulfoxide substituted for β-estradiol.

Microarray analysis

Isolation of total RNA, cDNA synthesis, cRNA labeling with the IVT Labeling Kit, and hybridization on the *Arabidopsis* ATH1 genome arrays were performed following the manufacturer's instructions (Affymetrix). Two biological replicates were tested for each treatment. The Affymetrix microarray suite software package (MAS 5.0) was used to scan and obtain signals. MAS-generated data files (.CEL files) were used as the input for preprocessing using the software package RMA to summarize probe sets and normalize signal intensities (Bolstad et al., 2003). Further analysis and filtering was performed using GeneSpring (Agilent). All samples were normalized per chip to the fiftieth percentile and per gene to median signals. For the Affymetrix flags, we filtered on 'present' value to appear in at least one sample. This reduced 22,746 total probe sets to 15,690 probe sets. The minimum expression value was set to 0.5 (log scale). Confidence in replicates was tested using standard deviation test with GeneSpring's default cross-gene error model turned on. The filter for *P*-values was set to 0.01. One-color data with deviation from one as an error model gave an average base/proportional of 34.94. First, we compared the transcriptomes in pER22-AGL24 induced by estradiol relative to mock-treatment. Second, we compared the transcriptomes in estradiol-induced pER22-AGL24 relative to those in estradiol-induced wild-type seedlings. Only genes showing consistently altered expression (fold change ⩾1.1) in these two comparisons were chosen as putative *AGL24*-regulated genes. The complete microarray data set is available as the accession number GSM6954 in the Gene Expression Omnibus (http://www.ncbi.nlm.nih.gov/geo).

ChIP assay

About 300 mg of 9-day-old *35S:AGL24-6HA* and *35S:SOC1-9myc* seedlings were fixed at 4°C for 40 minutes in 1% formaldehyde under vacuum. Fixed tissues were homogenized, and chromatin was isolated and sonicated to produce DNA fragments shorter than 500 bp. The solubilized chromatin was incubated with anti-HA agarose beads (Sigma) for 90 minutes at 4°C or used as an input control. Beads were washed five times with IP buffer (50 mM HEPES, pH 7.5, 150 mM KCl, 5 mM $MgCl_2$, 10 μM

Table 1. Primer pairs used for ChIP assays

Primer pair	Sequence (5′ to 3′)
For ChIP assays of protein binding on the *SOC1* sequence	
1	GGATGCAACCTCCTTTCATGAG, ATATGGGTTTGGTTTCATTTGG
2	AAAAACCTAACCAGGAGGAAGC, CTTCTTCTCCCTCCAGTAATGC
3	GCAAAAGAAGTAGCTTTCCTCG, AGCAGAGAGAGAAGAGACGAGTG
4	TGGACGCTTGAAACCTCATCCT, GGGAGGGAAAAAGATGTGTATG
5	AGTTGGATGGAAATGCCTGTCA, TTACAAGTGGGGGCATATAGGT
6	TCTCGTACCTATATGCCCCCACT, TTTATCTGTTGGGATGGAAAGA
7	GAGGCTAGTACAGAGACAATGG, GACCAAAAATAGCAAATGCCTC
8	TATATCGGGAGGAGGACCACAC, ATCCATACAGATTTTCGGACCT
9	ATCACATCTCTTTGACGTTTGCTT, GCCCTAATTTTGCAGAAACCAA
10	TGTTTCAGACATTTGGTCCATTTG, AGTCTTGTACTTTTTCCCCCTATTTTAG
ACTIN	CGTTTCGCTTTCCTTAGTGTTAGCT, AGCGAACGGATCTAGAGACTCACCTTG
For ChIP assays of protein binding on the *AGL24* sequence	
1	ACAAGTTCGAAATTTGGGCCA, TTCACGTTTTACCATTTGCCGT
2	TGCTGTTCATCAGTTCATCTACC, CTTATCAGGTGTCGCATCTAG
3	ATCCCCAATCATACCAAGTGAC, GTACTGGGAAATAAGAGAGCAG
4	AGTTCAATCCATCAAGATCCTCTC, TCTTTGGTAGACCTACTGAACA
ACTIN	CGTTTCGCTTTCCTTAGTGTTAGCT, AGCGAACGGATCTAGAGACTCACCTTG
For ChIP assays of protein binding on the *AP1* and *LFY* sequences	
AP1-1	CAAGTATCTTCTCCATACTGATC, TTATAAAGGTATCATAGAGATCGG
AP1-2	GAGTTAATTCTTTTTATGGATCCC, CATGTTTTGCAAATCTAAGCAAAG
AP1-3	GCAGTAGTGAATAATTAGGGCAA, AAGTTGCTCTTGTTGTCTTCTCCC
AP1-4	GTACGCAGGATTTAAGGAAAGAG, GATTTTTGTCCTGATCATCTACAAC
AP1-5	TTTGGTGTTTTCCACGTGTCTTC, ATAATACCGTAAGCAATAGTTGC
LFY-1	CTATACGACGTCGTTTGAAAGGGATCC, GCGTTTATATCTTCTCGGTCAGCCCA
LFY-2	TATCTTCCCCTAACAATACTTCCAAAGC, TCTTTGCAGAAGCCCGATAAGTTACT
ACTIN	CGTTTCGCTTTCCTTAGTGTTAGCT, AGCGAACGGATCTAGAGACTCACCTTG

$ZnSO_4$, 1% Triton X-100, 0.05% SDS), and then incubated with elution buffer (50 mM Tris, pH 8.0, 1% SDS, 10 mM EDTA) for 30 minutes at 65°C. The supernatant was collected and co-immunoprecipitated DNA was recovered according to a published protocol (Wang et al., 2002). An unrelated DNA sequence from the *ACTIN2/7* (*ACTIN*) gene that is constitutively expressed in *Arabidopsis* was used as an internal control for normalization (Johnson et al., 2002). Primer sequences used for the ChIP enrichment test are listed in Table 1. All ChIP assays were repeated at least twice and representative data are presented. For identification of the precise binding sites of AGL24 and SOC1, DNA enrichment was evaluated by real-time quantitative PCR in triplicate. Relative enrichment of each fragment was calculated first by normalizing the amount of a target DNA fragment against the *ACTIN* fragment, and then by normalizing the value for transgenic plants against the value for wild type as a negative control using the following equation: $2(^{Ct}_{\text{Transgenic Input}} - ^{Ct}_{\text{Transgenic ChIP}})/2(^{Ct}_{\text{WT Input}} - ^{Ct}_{\text{WT ChIP}})$.

Quantitative real-time PCR and semi-quantitative PCR

Total RNAs were extracted using the RNeasy Plant Mini Kit (Qiagen) and reverse-transcribed using the ThermoScript RT-PCR System (Invitrogen). Quantitative real-time PCR was performed in triplicate as previously described (Liu et al., 2007). The relative fold change was eventually calculated based on both Ct value and primer efficiency according to a published protocol (Pfaffl, 2001). Semi-quantitative PCR was performed as previously described (Yu et al., 2002). Primer sequences used for gene expression analyses are listed in Table 2.

In situ hybridization and GUS expression analysis

Non-radioactive in situ hybridization and GUS staining were carried out as previously described (Jefferson et al., 1987; Liu et al., 2007).

RESULTS

Generation of an estradiol-inducible *AGL24* system

To identify target genes that are regulated by *AGL24* during floral transition, we generated a functional pER22-*AGL24* transgenic line in which overexpression of *AGL24* is controlled by an estradiol-induced XVE system (Zuo et al., 2000). To test the dose response of the XVE inducible system, we examined the time-course of *AGL24* expression in seedlings from a selected transgenic pER22-*AGL24* line at different developmental stages (3, 6, 9, 12 and 15 days after

Table 2. Primer pairs used for gene expression analysis

Gene amplified	Sequence (5′ to 3′)
For quantitative real-time PCR	
AGL24	GAGGCTTTGGAGACAGAGTCGGTGA, AGATGGAAGCCCAAGCTTCAGGGAA
SOC1	AGCTGCAGAAAACGAGAAGCTCTCTG, GGGCTACTCTCTTCATCACCTCTTCC
AP1	CATGGGTGGTCTGTATCAAGAAGAT, CATGCGGCGAAGCAGCCAAGGTT
TUB2	AAGGACCTACTTCGGTGATGAG, GCTCTCCACCAATGTTAAGATGAG
For semi-quantitative PCR	
AGL24	AAGGAAGTCGAAGACAAAACCAAGC, TCTTATTCTCATCCACCAATTCCGA
TUB2	ATCCGTGAAGAGTACCCAGAT, TCACCTTCTTCATCCGCAGTT

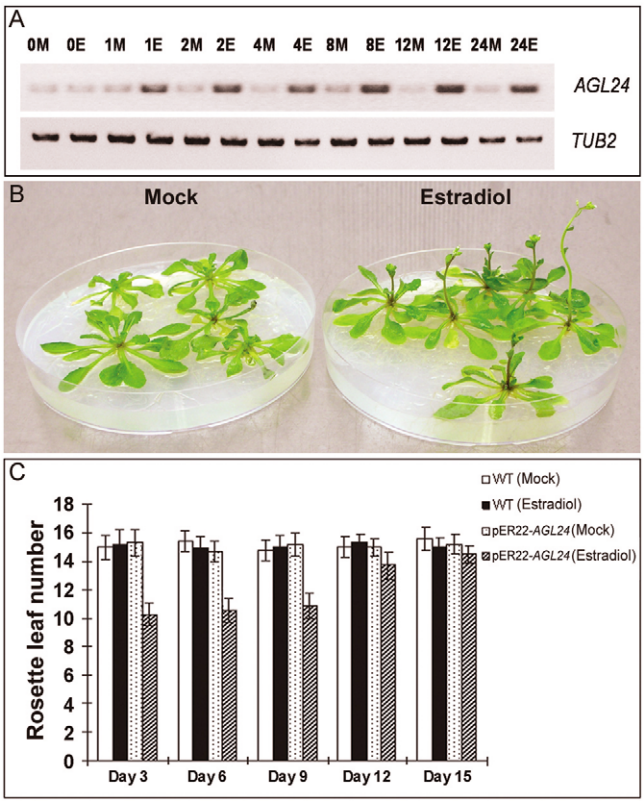

Fig. 1. Generation of a functional estradiol-inducible *AGL24* expression system. (**A**) Induction of *AGL24* expression in 9-day-old pER22-*AGL24 Arabidopsis* seedlings mock-treated (M) or treated with 10 μM β-estradiol (E) for 0, 1, 2, 4, 8, 12 or 24 hours. *TUB2* expression was used as a control. (**B**) The estradiol-inducible *AGL24* system is biologically functional. The pER22-*AGL24* plants (right) initially treated with β-estradiol at 9 days after germination show earlier flowering than mock-treated plants (left). (**C**) Upregulation of *AGL24* during floral transition is sufficient to promote flowering. β-estradiol treatment did not affect the flowering of wild-type plants, whereas initial treatment of pER22-*AGL24* with β-estradiol before or at the floral transitional stage (3, 6 or 9 days after germination) accelerated flowering.

germination) after they were transferred into Murashige and Skoog (MS) liquid medium supplemented with 10 μM β-estradiol. The XVE system proved to be a potent and reliable inducible system, as pER22-*AGL24* plants demonstrated consistent induction of *AGL24* expression irrespective of the developmental stage of the tested seedlings (data not shown). Fig. 1A shows an example of induction of *AGL24* expression in transgenic pER22-*AGL24* seedlings at 9 days after germination, in which *AGL24* induction nearly reached a maximal level after 8 hours of β-estradiol treatment and remained saturated thereafter.

We further applied continuous β-estradiol treatment on pER22-*AGL24* seedlings at different developmental stages to test the biological effects of *AGL24* induction (Fig. 1B,C). The pER22-*AGL24* seedlings initially treated with β-estradiol at the vegetative stage (3 and 6 days after germination) showed comparable flowering time to those initially treated at the floral transitional stage (9 days after germination). They flowered much earlier than the mock-treated transformants and wild-type seedlings (Fig. 1C). However, pER22-*AGL24* seedlings initially treated with β-estradiol at 12 and 15 days after germination did not flower significantly earlier than other seedlings (Fig. 1C). Thus, the selected pER22-*AGL24* line is biologically functional, and upregulation of *AGL24* to a certain threshold level during floral transition is responsible for promoting flowering.

SOC1 is induced by *AGL24*

We then chose 9-day-old pER22-*AGL24* seedlings at the floral transitional stage to investigate the change in transcriptomes responding to the induced *AGL24* expression. As *AGL24* induction reached a steady maximal level 8 hours after β-estradiol treatment (Fig. 1A), we collected seedlings at this time point for microarray analyses. Statistical analysis of the microarray data revealed 97 *AGL24*-downregulated genes and 87 *AGL24*-upregulated genes (see Table S1 in the supplementary material), among which *SOC1*, a flowering pathway integrator, was one of the genes activated by *AGL24*.

In pER22-*AGL24* seedlings treated with estradiol, *AGL24* expression was continuously induced, whereas *SOC1* expression was gradually upregulated up to 12 hours of induction, after which it was dramatically increased (Fig. 2A). This result, together with a previous observation that overexpression of *AGL24* affected *SOC1* expression in *FLC*-dependent and late flowering backgrounds (Michaels et al., 2003), indicates that *AGL24* affects *SOC1* expression under certain conditions. In wild-type plants grown in soil, *AGL24* expression was increased at 7 days after germination and was dramatically upregulated during floral transition, which was marked by significantly increased *AP1* expression from 9 days after germination (Fig. 2C, Fig. 5A). *SOC1* expression was gradually elevated in wild-type seedlings after germination and significantly increased from 9 days after germination, whereas its upregulation was delayed in *agl24-1* during floral transition (Fig. 2B). *SOC1* expression was much more elevated in *35S:AGL24* than in wild-type seedlings after 9 days post-germination (Fig. 2B). We further dissected developing *agl24-1* and wild-type seedlings to detect the change in *SOC1* expression in the leaf (cotyledon and rosette leaf) and the aerial part without leaf, including the shoot apex and young leaf primordia (Fig. 2D). *SOC1* expression was slightly altered in the leaf of *agl24-1*, whereas its expression in the aerial part without leaf of *agl24-1* was significantly reduced. In situ hybridization further revealed the reduced *SOC1* expression mainly at the shoot apex of *agl24-1* during floral transition (Fig. 2E). Thus, *AGL24* mainly upregulates *SOC1* at the shoot apex during floral transition, which is in accordance with the observation that upregulation of *AGL24* in floral transition is responsible for accelerating flowering (Fig. 1C).

AGL24-6HA binds directly to the *SOC1* promoter

To examine whether AGL24 directly controls *SOC1* transcription, we performed ChIP assays using a functional transgenic line expressing an AGL24-6HA fusion protein driven by the CaMV 35S promoter. By examining the phenotypes and genetic segregation ratios, we isolated one transgenic line containing a single insertion of the *35S:AGL24-6HA* transgene, which showed comparable flowering time to *35S:AGL24* (Fig. 3A,D). A notable floral phenotype relevant to *AGL24* function in promoting inflorescence identity is the generation of secondary flowers from a primary floral meristem when *AGL24* is overexpressed (Yu et al., 2004), a phenotype which was also observed in the selected *35S:AGL24-6HA* plant (Fig. 3C). These observations suggest that the fusion protein of AGL24-6HA retains the same biological function as AGL24.

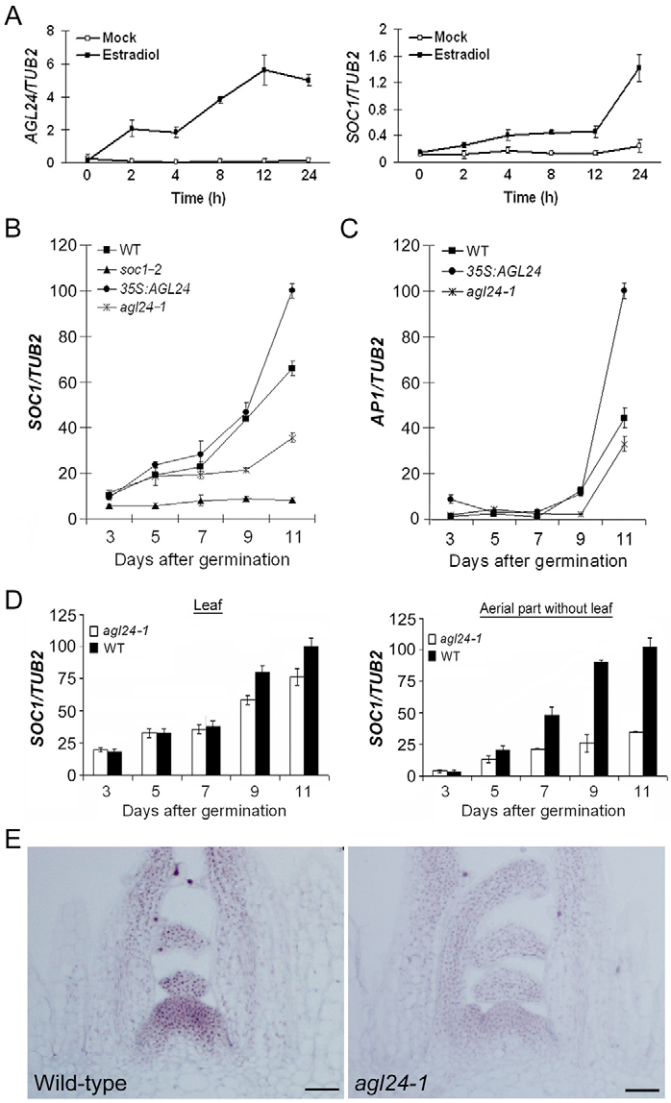

Fig. 2. *SOC1* expression is upregulated by *AGL24* during floral transition. (**A**) Induced expression of *AGL24* (left) and *SOC1* (right) in 9-day-old pER22-*AGL24 Arabidopsis* seedlings treated with β-estradiol or mock-treated for 0, 2, 4, 8, 12 and 24 hours. (**B**,**C**) Relative temporal expression of *SOC1* (B) and *AP1* (C) in developing seedlings with different genetic background under long-day conditions. (**D**) Relative temporal expression of *SOC1* in the aerial part without leaf and leaf of *agl24-1* and wild-type seedlings. Transcript levels in A-D were determined by quantitative real-time PCR analyses of three independently collected samples. Results were normalized against the expression of *TUB2*. Error bars indicate s.d. (**E**) In situ localization of *SOC1* at the shot apex of 11-day-old *agl24-1* and wild-type seedlings. For the purpose of comparing signals, sections of these plants were placed on the same slides for hybridization and detection. Scale bars: 25 μm.

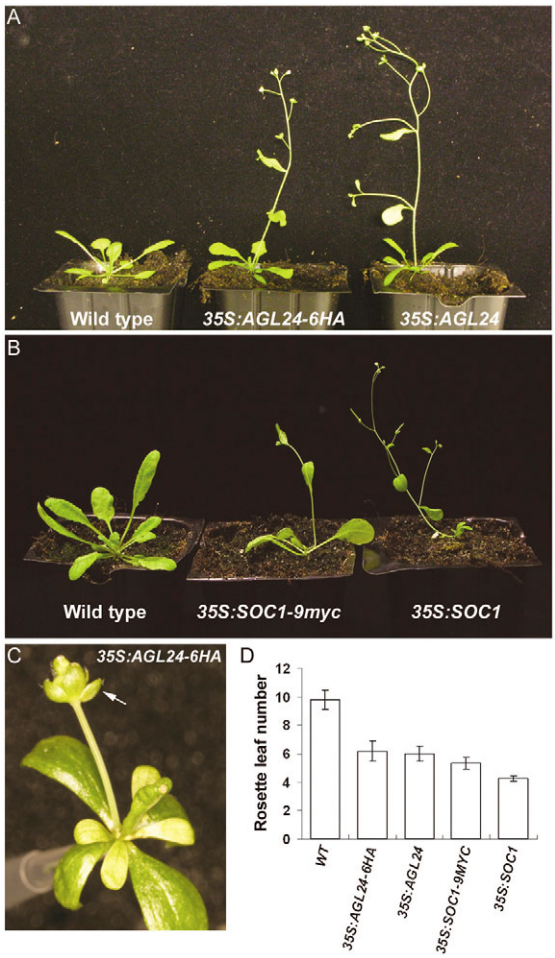

Fig. 3. Generation of functional *35S:AGL24-6HA* and *35S:SOC1-9myc* transgenic lines. (**A**) *35S:AGL24-6HA* and *35S:AGL24 Arabidopsis* plants show early flowering under long-day conditions. (**B**) *35S:SOC1-9myc* and *35S:SOC1* plants show early flowering under long-day conditions. (**C**) An ectopic secondary flower (arrow) is observed in a *35S:AGL24-6HA* flower. (**D**) Flowering time of generated transgenic lines under long-day conditions. Number of rosette leaves represents flowering time. Values representing the mean±s.d. were scored from at least 20 plants of each genotype.

We scanned the *SOC1* genomic sequence for CArG motifs with a maximum one nucleotide mismatch, and designed ten pairs of primers near the identified motifs for measurement of DNA enrichment by quantitative real-time PCR (Fig. 4A). The number 6 genomic fragment (–1260 to –1133, relative to the translation start site) containing one CArG motif showed the strongest enrichment of around 6-fold (Fig. 4B), suggesting that AGL24-6HA binds directly to this site in vivo.

Effect of mutagenesis of the AGL24 binding site in the *SOC1* promoter

To evaluate whether the CArG motif within the number 6 fragment is responsible for the upregulation of *SOC1* during floral transition, we transcriptionally fused a *SOC1* 5′ upstream sequence to the *GUS* reporter gene (Fig. 4C). This upstream sequence included a 1.4 kb *SOC1* promoter upstream of the *SOC1* transcription start site, because a *SOC1* genomic fragment including this promoter is sufficient to complement *soc1* mutation (Samach et al., 2000). Based on this construct, we created another reporter gene cassette in which the putative AGL24 binding site was mutated (Fig. 4C). Among 24 independent lines of transformants harboring Pro_{SOC1}*:GUS*, 20 lines displayed strong GUS staining during floral transition (Fig. 4D,E), whereas among 18 lines of the transformants harboring the construct with the mutated AGL24 binding site, 11 lines displayed intermediate GUS staining (Fig. 4D,E). It is noteworthy that the difference in GUS staining conferred by Pro_{SOC1}*:GUS* and its mutated form was most apparent at the shoot apex. These

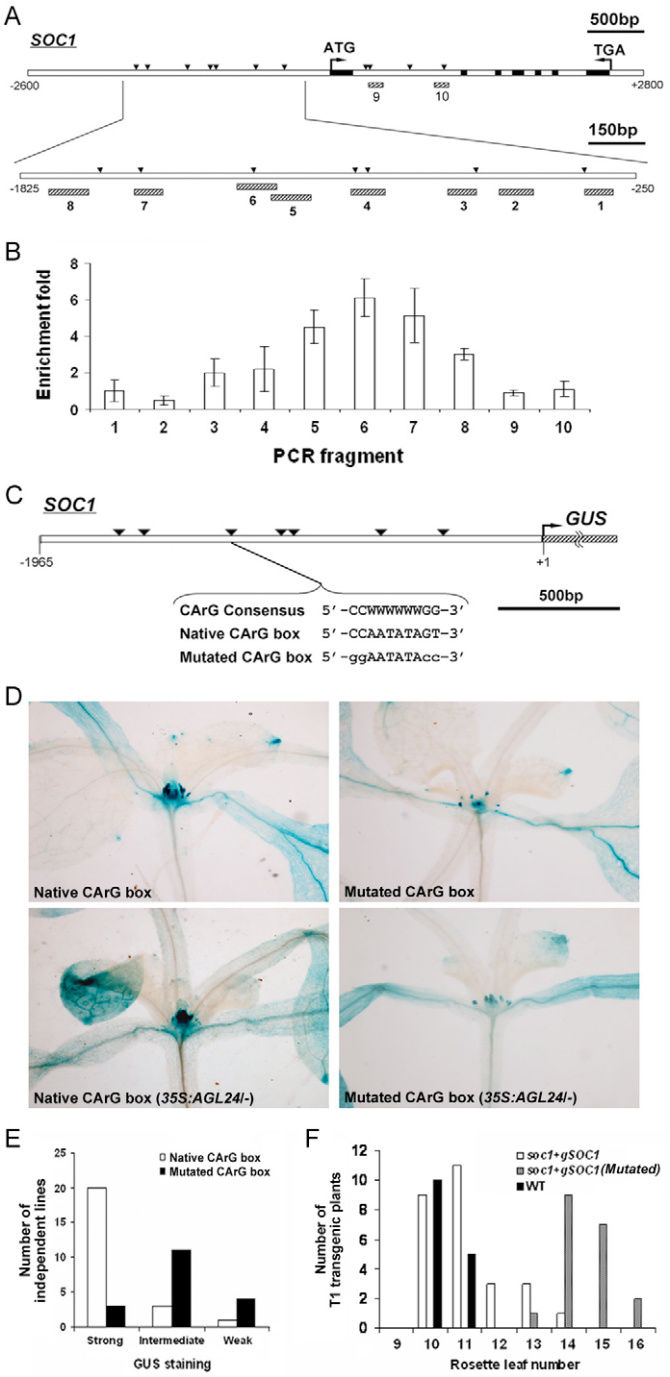

Fig. 4. *AGL24* directly regulates *SOC1*. (**A**) Schematic of the *Arabidopsis SOC1* genomic region. Black boxes, exons; white boxes, introns and upstream regions. Bent arrows denote translation start sites and stop codons. Arrowheads indicate the sites containing either single mismatch or perfect match with the consensus binding sequence (CArG box) of MADS-domain proteins. Ten PCR fragments corresponding to the DNA sequences near these CArG boxes were designed for ChIP analysis. (**B**) ChIP enrichment test by quantitative real-time PCR shows the binding of AGL24-6HA to the region near the number 6 fragment. (**C**) Schematic of the Pro_{SOC1}*:GUS* construct. The native CArG box within the number 6 fragment identified in B was mutated as indicated. (**D**) GUS staining of Pro_{SOC1}*:GUS* plants. Representative GUS staining of 12-day-old transformants containing Pro_{SOC1}*:GUS* and its mutated form is shown in the upper panels. Representative lines were crossed with *35S:AGL24*, and GUS staining of 10-day-old F1 plants is shown in the lower panels. (**E**) Distribution of relative GUS staining intensity in the transformants containing Pro_{SOC1}*:GUS* and its mutated construct. (**F**) Distribution of flowering time in T1 transgenic plants carrying the wild-type *SOC1* gene and its mutated form in the *soc1-2* mutant background.

observations, which are consistent with the different expression of *SOC1* at the shoot apex of wild-type and *agl24-1* seedlings, demonstrate that the tested AGL24 binding site is responsible for upregulating *SOC1* expression at the shoot apex during floral transition. We further crossed the transformants harboring Pro_{SOC1}*:GUS* and its mutated construct with *35S:AGL24*, and examined the change in GUS staining in response to the increased *AGL24* activity. In the *35S:AGL24* background, GUS staining of both Pro_{SOC1}*:GUS* and its mutated form slightly increased in the leaf compared with that in wild-type plants (Fig. 4D). By contrast, GUS staining of Pro_{SOC1}*:GUS* at the shoot apex of *35S:AGL24* during floral transition increased compared with that in the wild-type background (Fig. 4D), whereas staining of the mutated construct remained lower at the shoot apex of *35S:AGL24* than in wild type (Fig. 4D). Thus, mutation of the AGL24 binding site almost completely abolishes upregulation of *SOC1* by *AGL24* at the shoot apex, corroborating that AGL24 specifically binds to this site to promote *SOC1* expression at the shoot apex during floral transition.

To confirm that the AGL24 binding site is essential for *SOC1* function in flowering, *soc1-2* was transformed with either a genomic *SOC1* construct or its derived construct with the mutated AGL24 binding site. The average flowering time of *soc1-2* mutants transformed with the *SOC1* genomic construct, which comprised 1.97 kb of 5′ upstream sequence (Fig. 4C) and the full gene coding region plus introns, was around 11.1 rosette leaves (Fig. 4F). This was comparable with the average flowering time of wild-type plants (10.3 rosette leaves), but was earlier than that of *soc1-2* mutants transformed with the mutated *SOC1* construct (14.5 rosette leaves) (Fig. 4F). These results substantiate that the AGL24 binding site is important for *SOC1* function in promoting flowering.

SOC1-9myc binds directly to the *AGL24* and *LFY* promoters

Since *AGL24* expression is also affected by *SOC1* (Michaels et al., 2003; Yu et al., 2002), we quantitatively examined the effect of *SOC1* on *AGL24* expression. *AGL24* expression was increased in wild-type seedlings from 5 days after germination, whereas its upregulation was delayed in *soc1-2* (Fig. 5A). In *35S:SOC1*, *AGL24* expression was high in seedlings 3 and 5 days after germination, and reduced thereafter (Fig. 5A). *AP1* expression was notably higher in *35S:SOC1* than in wild-type seedlings and its expression in *35S:SOC1* 5 days after germination was almost comparable with that in wild-type seedlings 11 days after germination (Fig. 5B). As *AGL24* expression is repressed by induced *AP1* activity (Yu et al., 2004), *AGL24* expression in *35S:SOC1* may reflect a combined effect of repression of *AGL24* by *AP1* and promotion of *AGL24* by overexpression of *SOC1*.

We also dissected developing *soc1-2* and wild-type seedlings to detect the change in *AGL24* expression in the leaf and aerial part without leaf (Fig. 5C). In wild-type seedlings, *AGL24* expression in the leaf was much lower than that in the aerial part without leaf (data

not shown). Compared with its expression in wild-type tissues, *AGL24* expression only slightly decreased in the leaf of *soc1-2*, whereas its expression in the aerial part without leaf of *soc1-2* was significantly reduced during floral transition. Thus, *SOC1* upregulates *AGL24* mainly at the shoot apex during floral transition.

We further tested whether *SOC1* could directly regulate *AGL24* by ChIP assays using a functional line harboring a *SOC1-9myc* fusion transgene driven by the CaMV 35S promoter (Fig. 3B,D). The number 1 genomic fragment (–2125 to –1987, relative to the translation start site) that lies near two CArG motifs, each with one nucleotide mismatch, was enriched by about 5-fold (Fig. 5D,E), suggesting that SOC1-9myc binds directly to the *AGL24* genomic region in vivo.

Using the same ChIP approach, we tested whether SOC1-9myc and AGL24-6HA could bind directly to the genomic sequences of two floral meristem identity genes, *AP1* and *LFY*. Our results

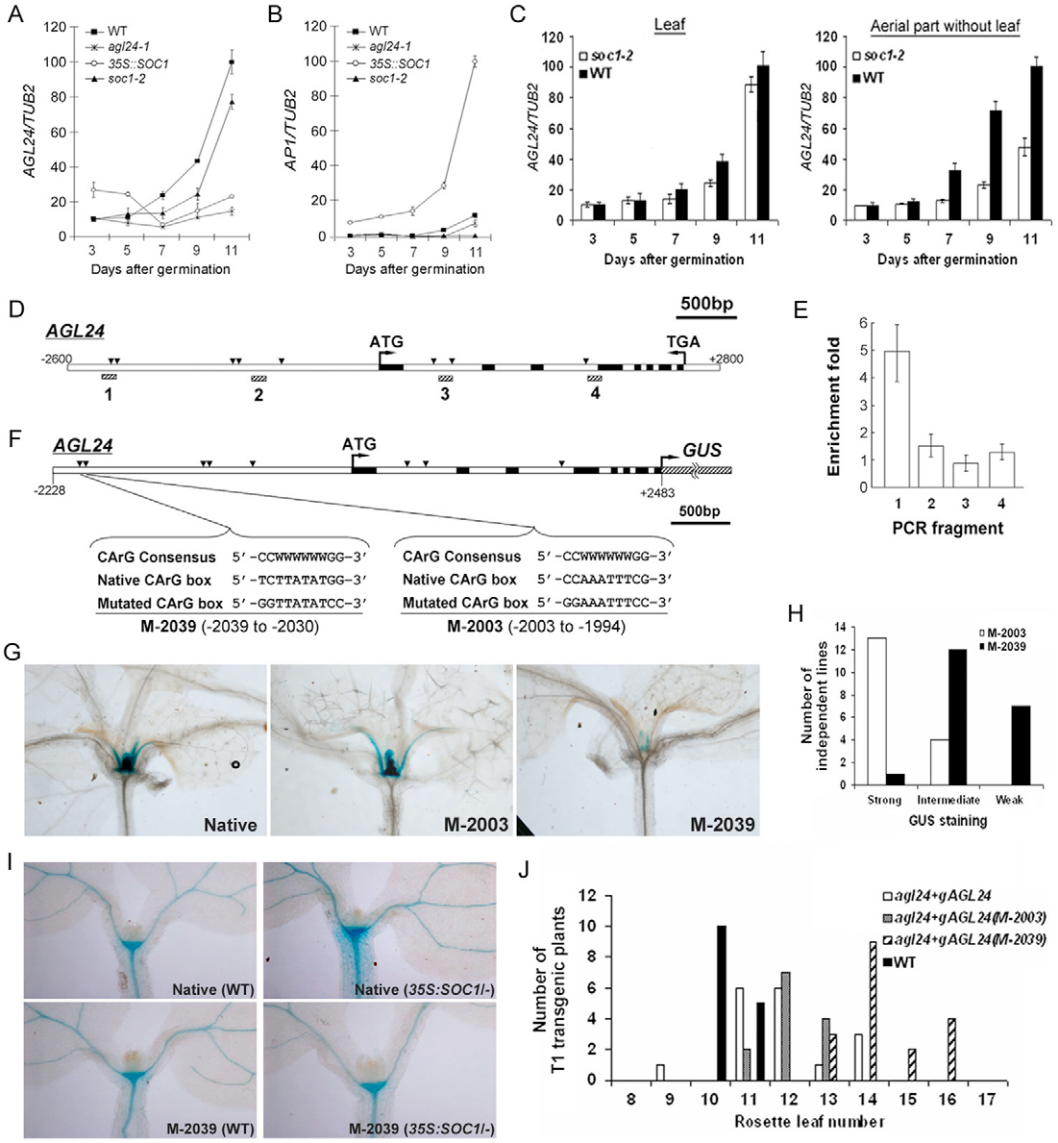

Fig. 5. *SOC1* directly regulates *AGL24*. (**A**,**B**) Relative temporal expression of *AGL24* (A) and *AP1* (B) in developing *Arabidopsis* seedlings of different genetic background under long-day conditions. (**C**) Relative temporal expression of *AGL24* in the aerial part without leaf and leaf of *soc1-2* and wild-type seedlings. Transcript levels in A-C were determined by quantitative real-time PCR analyses of three independently collected samples. Results were normalized against the expression of *TUB2*. Error bars indicate s.d. (**D**) Schematic of the *AGL24* genomic region. Arrowheads indicate the sites containing either single mismatch or perfect match with the consensus binding sequence (CArG box) of MADS-domain proteins. Four PCR fragments corresponding to the DNA sequences near these CArG boxes were designed for ChIP analysis. (**E**) ChIP enrichment test shows the binding of SOC1-9myc to the region near the number 1 fragment indicated in D. (**F**) Schematic of the Pro_{AGL24}*:GUS* construct. Two native CArG boxes within the number 1 fragment identified in D and E were mutated as indicated. (**G**) Representative GUS staining in 12-day-old transformants containing Pro_{AGL24}*:GUS* and its derived constructs with the mutated CArG boxes (M-2003 and M-2039). (**H**) Distribution of relative GUS staining intensity in the transformants containing M-2003 and M-2039. (**I**) GUS staining of Pro_{AGL24}*:GUS* and M-2039 in the wild-type (left) and *35S:SOC1* (right) background. Representative lines of transformants containing Pro_{AGL24}*:GUS* and M-2039 were crossed with *35S:SOC1*, and GUS staining of 4-day-old F1 plants is shown on the right. (**J**) Distribution of flowering time in T1 transgenic plants carrying the wild-type *AGL24* gene and its mutated forms (M-2003 and M-2039) in the *agl24-1* mutant background.

showed that only one fragment near a CArG motif in the *LFY* promoter was enriched by anti-myc antibody in *SOC1-9myc* plants (Fig. 6), suggesting that SOC1-9myc binds directly to the *LFY* promoter in vivo. In addition, we found that SOC1-9myc and AGL24-6HA did not bind directly to their own genomic sequences (see Fig. S1 in the supplementary material).

Effect of mutagenesis of the SOC1 binding site in the *AGL24* promoter

To identify the precise CArG motif that is responsible for the upregulation of *AGL24* by *SOC1*, we used an established Pro_{AGL24}*:GUS* reporter line in which an *AGL24* genomic fragment containing 4.7 kb of sequence upstream of the stop codon was translationally fused with the *GUS* reporter gene (Liu et al., 2007). The *GUS* expression in this line is similar to that of endogenous *AGL24* expression. Based on this Pro_{AGL24}*:GUS* construct, we generated two reporter gene cassettes, M-2003 and M-2039, in which one or other of two CArG motifs within the number 1 genomic fragment were mutated (Fig. 5F). Among 17 independent lines of the transformants bearing the M-2003 mutation (Fig. 5G,H), 13 lines exhibited strong GUS staining, which was comparable with that conferred by the Pro_{AGL24}*:GUS* construct. By contrast, the majority of 20 independent lines of the transformants bearing the M-2039 mutation exhibited intermediate or weak GUS staining (Fig. 5G,H). The difference in the GUS staining of wild-type, M-2003 and M-2039 plants was most apparent at the shoot apex. These results, together with differential expression of *AGL24* in *soc1-2* and wild-type plants, strongly suggest that SOC1 mainly binds to the CArG motif of M-2039 to upregulate *AGL24* expression at the shoot apex during floral transition.

We further crossed the transformants harboring Pro_{AGL24}*:GUS* and its mutated construct M-2039 with *35S:SOC1*, and examined the change in GUS staining in response to the increased *SOC1* activity. As *35S:SOC1* showed very early flowering (Lee et al., 2000; Samach et al., 2000) and *AGL24* was only upregulated at early developmental stages of *35S:SOC1* (Fig. 5A), we compared GUS staining in 4-day-old seedlings. GUS staining of 4-day-old Pro_{AGL24}*:GUS* and M-2039 seedlings did not reveal any difference in wild-type background (Fig. 5I), which was consistent with unaltered *AGL24* expression in *soc1-2* and wild-type seedlings at a similar developmental stage (Fig. 5A). However, GUS staining of Pro_{AGL24}*:GUS* at the shoot apex and hypocotyl of *35S:SOC1* was increased compared with that in the wild-type background, whereas staining of M-2039 remained the same in *35S:SOC1* as in wild type (Fig. 5I). Thus, mutation of the SOC1 binding site indeed compromises upregulation of *AGL24* in young seedlings.

To confirm that the revealed SOC1 binding site is essential for *AGL24* function in flowering, *agl24-1* was transformed with either a genomic *AGL24* construct or its derived construct with the M-2003 or M-2039 mutation. The average flowering time of *agl24-1* mutants transformed with the *AGL24* genomic construct, which comprised 2.23 kb of 5′ upstream sequence (Fig. 5F) and the full gene coding region plus introns, was around 11.9 rosette leaves (Fig. 5J). This was comparable to the average flowering time of *agl24-1* mutants transformed with the M-2003 mutation (12.2 rosette leaves), but was earlier than that of *agl24-1* mutants transformed with the M-2039 mutation (14.4 rosette leaves) (Fig. 5J). These results substantiate that the SOC1 binding site at M-2039 is important for *AGL24* function in promoting flowering.

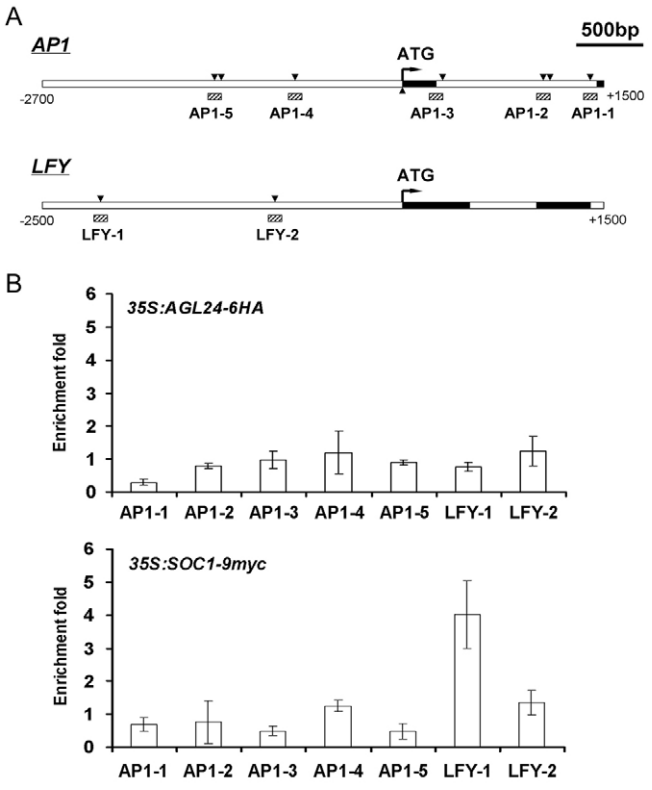

Fig. 6. ChIP analysis of the binding of AGL24-6HA and SOC1-9myc to the *AP1* and *LFY* genomic regions. (**A**) Schematic of the *Arabidopsis AP1* and *LFY* genomic regions. Arrowheads indicate the sites containing either single mismatch or perfect match with the consensus binding sequence (CArG box) of MADS-domain proteins. The hatched boxes represent the DNA fragments near CArG box(es) amplified in ChIP assays. (**B**) ChIP enrichment test shows the binding of SOC1-9myc to the *LFY* genomic region.

Interaction of *AGL24* and *SOC1* mediates the effect of gibberellins on flowering

Previous studies have revealed that the expression of *AGL24* and *SOC1* is differently controlled by the photoperiod, autonomous and vernalization pathways (Michaels et al., 2003; Yu et al., 2002). Although it has been shown that GA could affect the expression of *AGL24* and *SOC1* (Lee et al., 2000; Moon et al., 2003; Yu et al., 2002), it remains elusive how the GA pathway regulates their expression. We examined the expression of both genes in the wild-type and mutant seedlings grown under short-day conditions. In the wild-type seedlings, the expression of *AGL24* and *SOC1* gradually increased under mock treatment and their expression was upregulated upon GA treatment (Fig. 7A,B), confirming that both genes are targets of the GA pathway (Lee et al., 2000; Moon et al., 2003; Yu et al., 2002). In *agl24-1* and *soc1-2*, the respective upregulation of *SOC1* and *AGL24* was nearly abolished upon GA treatment (Fig. 7A,B). This suggests that upregulation of *SOC1* and *AGL24* in response to GA is mediated by *AGL24* and *SOC1*, respectively. Under long-day conditions, GA treatment did not promote flowering in wild type or mutants, indicating that signals from other flowering genetic pathways play major roles in regulating flowering time (Fig. 7C). During our experimental period, *soc1-2 agl24-1* did not flower under short-day conditions without GA treatment, which was significantly different from the flowering phenotype exhibited by either of the single mutants (Fig. 7D). Upon GA treatment, flowering of wild type, *soc1-2* and *agl24*-1 was accelerated, whereas *soc1-2 agl24-1* still flowered extremely late

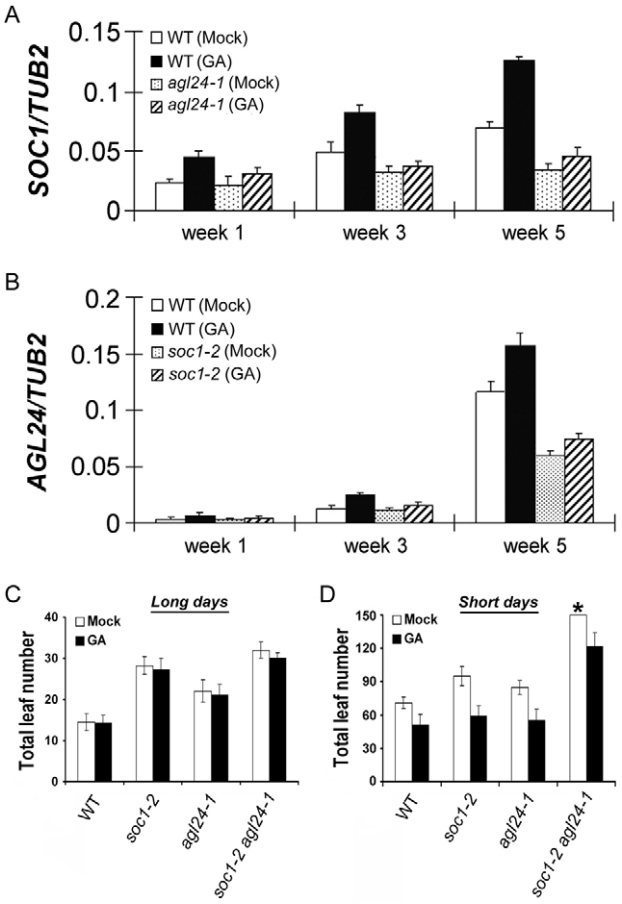

Fig. 7. Gibberellin (GA) regulates flowering time through independently controlling *AGL24* and *SOC1*. (**A**) Temporal expression of *SOC1* in wild-type and *agl24-1 Arabidopsis* seedlings with or without GA treatment under short-day conditions. (**B**) Temporal expression of *AGL24* in wild-type and *soc1-2* seedlings with or without GA treatment under short-day conditions. Time points on the *x*-axis indicate the time of collection of plant materials after first GA treatment. Transcript levels in A and B were determined by quantitative real-time PCR analyses of three independently collected samples. Results were normalized against the expression of *TUB2*. Error bars indicate s.d. (**C**) Flowering time of *soc1-2* and *agl24-1* mutants with or without GA treatment under long-day conditions. (**D**) Flowering time of *soc1-2* and *agl24-1* mutants with or without GA treatment under short-day conditions. Number of total leaves represents flowering time in C and D. Values representing the mean±s.d. were scored from at least 20 plants of each genotype. Asterisk indicates that flowering was not observed in *soc1-2 agl24-1* under short-day conditions without GA treatment.

(Fig. 7D). These observations suggest that *SOC1* and *AGL24* upregulate each other in response to GA and synergistically determine flowering time under short-day conditions.

DISCUSSION

The transition to flowering involves multiple genetic pathways in response to developmental and environmental signals. Several global expression analyses have been performed to discover genes or pathways affecting floral induction (Schmid et al., 2003; Wigge et al., 2005; Wilson et al., 2005). In this study, we used an estradiol-inducible gene expression system in combination with microarray analysis to identify genes induced by the flowering promoter *AGL24* and identified *SOC1* as one of these induced genes. At the vegetative phase, *SOC1* expression remains low and is almost unaffected by altered *AGL24* activity, whereas upregulation of *SOC1* expression at the shoot apex during floral transition is highly dependent on *AGL24* activity (Fig. 2). ChIP assay revealed that AGL24-6HA can bind to the regulatory sequence of *SOC1*, and mutagenesis of the AGL24-6HA binding site reduces *SOC1* expression at the shoot apex (Fig. 4), demonstrating that *AGL24* directly regulates *SOC1* transcription specifically at the shoot apex during floral transition. These results, together with the observations that *AGL24* is significantly upregulated during floral transition and that induced *AGL24* expression during floral transition is sufficient to promote flowering (Fig. 1C, Fig. 5A), suggest that direct upregulation of *SOC1* by increased *AGL24* expression is an important molecular event during floral transition. On the other hand, several pieces of evidence have also shown that *AGL24* expression at the shoot apex is directly upregulated by *SOC1* (Fig. 5), suggesting that *AGL24* and *SOC1* regulate each other to provide positive-feedback control of their expression at the shoot apex during floral transition.

In *soc1* and *agl24* mutants, changes in *AGL24* and *SOC1* expression, respectively, still affect flowering time, implying that they might regulate different genes involved in flowering (Michaels et al., 2003; Yu et al., 2002). Our ChIP assay revealed that the *LFY* genomic sequence is only bound by SOC1-9myc, and not by AGL24-6HA (Fig. 6). This confirms that *AGL24* and *SOC1* control distinct genes, while they directly regulate each other.

A significant aspect of the mutual interaction between *AGL24* and *SOC1* is the integration of flowering signals from several genetic pathways (Fig. 8). The vernalization pathway regulates flowering through at least several different regulators. In a *FLC*-independent pathway, vernalization regulates the expression of at least two genes, *AGL24* (Michaels et al., 2003; Yu et al., 2002) and *AGL19* (Schonrock et al., 2006). In a *FLC*-dependent pathway, *FLC* plays a dual role in directly repressing *SOC1* transcription in the meristem and indirectly delaying *SOC1* expression by repression of *FT*, a systemic signal required for the activation of *SOC1*, in the leaf (Hepworth et al., 2002; Searle et al., 2006). Several recent studies have provided in vitro and in vivo data showing that FLC binds to a CArG box at the *SOC1* 5′ promoter (Helliwell et al., 2006; Hepworth et al., 2002; Searle et al., 2006). Nevertheless, vernalization can still upregulate *SOC1* expression in *flc* mutants under short-day conditions, indicating that *SOC1* is also regulated in a *FLC*-independent way (Moon et al., 2003). This can be partly explained by direct regulation of *SOC1* by *AGL24*.

The autonomous pathway promotes flowering by repressing *FLC* (Michaels and Amasino, 2001) and thus affecting *SOC1* expression. Although *AGL24* expression is not affected by *FLC*, its expression is significantly reduced in several mutants in the autonomous pathway, such as *fve*, *fpa* and *fca* (Michaels et al., 2003; Yu et al., 2002), suggesting that the autonomous pathway also upregulates *AGL24* in a *FLC*-independent way. Since FLC and AGL24 bind to distinct sites of the *SOC1* promoter region, it will be interesting to further elucidate the SOC1 transcription complex, in which AGL24 may compete with FLC in response to the signals from vernalization and autonomous pathways.

In the photoperiod pathway, *SOC1* is mainly regulated by *FT* and indirectly by *CO* via other unknown DNA-binding factor(s) (Hepworth et al., 2002; Lee et al., 2000; Samach et al., 2000; Yoo et al., 2005), whereas *AGL24* is affected by the activity of *CO*, but not

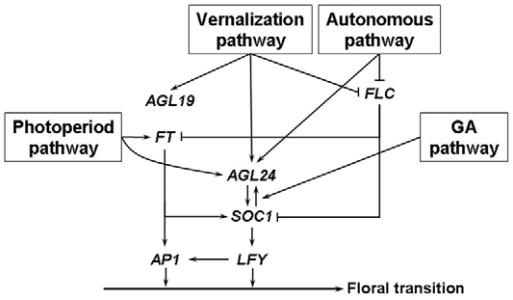

Fig. 8. Direct interaction between *AGL24* and *SOC1* mediates the integration of flowering signals in *Arabidopsis*. *AGL24* and *SOC1* directly regulate mutual mRNA expression at the shoot apex. This cross-regulation integrates flowering signals from four genetic pathways to promote the floral transition from vegetative to reproductive development. Arrows and bars represent promotion and repression effects, respectively.

of *FT* (Yu et al., 2002). Although *FT* has been suggested as a major output of *CO* (Samach et al., 2000; Wigge et al., 2005; Yoo et al., 2005), *FT* integrates other floral signals irrespective of *CO*. For example, *FLC* directly represses *FT* in the leaf, thus affecting its activation of *SOC1* (Helliwell et al., 2006; Searle et al., 2006). In addition, thermal induction of flowering by elevated growth temperature is also mediated by *FT* (Balasubramanian et al., 2006). Thus, positive regulation of *SOC1* by *FT* is only partially controlled by the photoperiod pathway. It is likely that direct regulation of *SOC1* by *AGL24*, which is regulated by *CO*, provides an alternative channel to enhance the effect of the photoperiod pathway on *SOC1* expression.

Under short-day conditions, the GA pathway is a major flowering pathway that mainly affects *SOC1*, but not *FLC* and *FT* (Moon et al., 2003). Removal of *FLC* repression only derepresses *SOC1* expression and is not sufficient to activate *SOC1* under short-day conditions, suggesting that GA activation of *SOC1* needs positive regulator(s) (Moon et al., 2003). *AGL24* is a possible regulator of *SOC1* in the GA pathway because *SOC1* and *AGL24* upregulate each other in response to GA, and loss of either gene compromises the effect of GA on the promotion of another gene (Fig. 7). In addition, flowering of overexpression of *SOC1* under short-day conditions is partially delayed in the GA-deficient mutant *ga1-3* (Moon et al., 2003), indicating that GA regulates other target(s) in addition to *SOC1*. Our results have identified that *AGL24* is another major target of the GA pathway as *soc1-2 agl24-1* double mutants do not flower under short-day conditions without GA treatment (Fig. 7D). Taken together, direct interaction of *AGL24* and *SOC1* allows a synergistic integration of environmental and endogenous signals from several upstream genetic pathways to promote flowering (Fig. 8).

Overall, the results presented here show that *AGL24* and *SOC1* directly upregulate each other at the shoot apex during floral transition. This integrates flowering signals perceived by these two regulators and provides positive-feedback regulation of their own expression to a quantitative threshold required for the transition of the shoot apical meristem from a vegetative to a reproductive state. Direct cross-regulation between *AGL24* and *SOC1* represents a novel regulatory mode for the transcription factors involved in the control of flowering time and further investigation of their target genes would provide a better understanding of the subtle regulatory hierarchy of floral transition.

We thank Nam-Hai Chua for providing the vector pER8; Dr Ilha Lee for the seeds of *soc1-2* and *35S:SOC1*; Drs Rick Amasino and Marty Yanofsky for *agl24-1*; and Drs Toshiro Ito, Frederic Berger and Yuehui He for critical reading of the manuscript. This work was supported by Academic Research Funds R-154-000-282-112 and R-154-000-337-112 from the National University of Singapore and R-154-000-263-112 from the Ministry of Education, Singapore, and the intramural research funds from Temasek Life Sciences Laboratory.

Supplementary material

Supplementary material for this article is available at http://dev.biologists.org/cgi/content/full/135/8/1481/DC1

References

Amasino, R. (2004). Vernalization, competence, and the epigenetic memory of winter. *Plant Cell* **16**, 2553-2559.
Balasubramanian, S., Sureshkumar, S., Lempe, J. and Weigel, D. (2006). Potent induction of Arabidopsis thaliana flowering by elevated growth temperature. *PLoS Genet.* **2**, e106.
Blazquez, M. A., Ahn, J. H. and Weigel, D. (2003). A thermosensory pathway controlling flowering time in Arabidopsis thaliana. *Nat. Genet.* **33**, 168-171.
Bolstad, B. M., Irizarry, R. A., Astrand, M. and Speed, T. P. (2003). A comparison of normalization methods for high density oligonucleotide array data based on variance and bias. *Bioinformatics* **19**, 185-193.
Boss, P. K., Bastow, R. M., Mylne, J. S. and Dean, C. (2004). Multiple pathways in the decision to flower: enabling, promoting, and resetting. *Plant Cell* **16 Suppl.**, S18-S31.
Cerdan, P. D. and Chory, J. (2003). Regulation of flowering time by light quality. *Nature* **423**, 881-885.
Clough, S. J. and Bent, A. F. (1998). Floral dip: a simplified method for Agrobacterium-mediated transformation of Arabidopsis thaliana. *Plant J.* **16**, 735-743.
Corbesier, L., Vincent, C., Jang, S., Fornara, F., Fan, Q., Searle, I., Giakountis, A., Farrona, S., Gissot, L., Turnbull, C. et al. (2007). FT protein movement contributes to long-distance signaling in floral induction of Arabidopsis. *Science* **316**, 1030-1033.
Gregis, V., Sessa, A., Colombo, L. and Kater, M. M. (2006). AGL24, SHORT VEGETATIVE PHASE, and APETALA1 redundantly control AGAMOUS during early stages of flower development in Arabidopsis. *Plant Cell* **18**, 1373-1382.
Halliday, K. J., Salter, M. G., Thingnaes, E. and Whitelam, G. C. (2003). Phytochrome control of flowering is temperature sensitive and correlates with expression of the floral integrator FT. *Plant J.* **33**, 875-885.
Helliwell, C. A., Wood, C. C., Robertson, M., James Peacock, W. and Dennis, E. S. (2006). The Arabidopsis FLC protein interacts directly in vivo with SOC1 and FT chromatin and is part of a high-molecular-weight protein complex. *Plant J.* **46**, 183-192.
Hepworth, S. R., Valverde, F., Ravenscroft, D., Mouradov, A. and Coupland, G. (2002). Antagonistic regulation of flowering-time gene SOC1 by CONSTANS and FLC via separate promoter motifs. *EMBO J.* **21**, 4327-4337.
Jefferson, R. A., Kavanagh, T. A. and Bevan, M. W. (1987). GUS fusions: beta-glucuronidase as a sensitive and versatile gene fusion marker in higher plants. *EMBO J.* **6**, 3901-3907.
Johnson, L., Cao, X. and Jacobsen, S. (2002). Interplay between two epigenetic marks. DNA methylation and histone H3 lysine 9 methylation. *Curr. Biol.* **12**, 1360-1367.
Lee, H., Suh, S. S., Park, E., Cho, E., Ahn, J. H., Kim, S. G., Lee, J. S., Kwon, Y. M. and Lee, I. (2000). The AGAMOUS-LIKE 20 MADS domain protein integrates floral inductive pathways in Arabidopsis. *Genes Dev.* **14**, 2366-2376.
Liu, C., Zhou, J., Bracha-Drori, K., Yalovsky, S., Ito, T. and Yu, H. (2007). Specification of Arabidopsis floral meristem identity by repression of flowering time genes. *Development* **134**, 1901-1910.
Michaels, S. D. and Amasino, R. M. (2001). Loss of FLOWERING LOCUS C activity eliminates the late-flowering phenotype of FRIGIDA and autonomous pathway mutations but not responsiveness to vernalization. *Plant Cell* **13**, 935-941.
Michaels, S. D., Ditta, G., Gustafson-Brown, C., Pelaz, S., Yanofsky, M. and Amasino, R. M. (2003). AGL24 acts as a promoter of flowering in Arabidopsis and is positively regulated by vernalization. *Plant J.* **33**, 867-874.
Moon, J., Suh, S. S., Lee, H., Choi, K. R., Hong, C. B., Paek, N. C., Kim, S. G. and Lee, I. (2003). The SOC1 MADS-box gene integrates vernalization and gibberellin signals for flowering in Arabidopsis. *Plant J.* **35**, 613-623.
Mouradov, A., Cremer, F. and Coupland, G. (2002). Control of flowering time: interacting pathways as a basis for diversity. *Plant Cell* **14 Suppl.**, S111-S130.
Parcy, F. (2005). Flowering: a time for integration. *Int. J. Dev. Biol.* **49**, 585-593.
Pfaffl, M. W. (2001). A new mathematical model for relative quantification in real-time RT-PCR. *Nucleic Acids Res.* **29**, e45.
Riechmann, J. L., Wang, M. and Meyerowitz, E. M. (1996). DNA-binding properties of Arabidopsis MADS domain homeotic proteins APETALA1, APETALA3, PISTILLATA and AGAMOUS. *Nucleic Acids Res.* **24**, 3134-3141.
Samach, A., Onouchi, H., Gold, S. E., Ditta, G. S., Schwarz-Sommer, Z., Yanofsky, M. F. and Coupland, G. (2000). Distinct roles of CONSTANS

target genes in reproductive development of Arabidopsis. *Science* **288**, 1613-1616.

Schmid, M., Uhlenhaut, N. H., Godard, F., Demar, M., Bressan, R., Weigel, D. and Lohmann, J. U. (2003). Dissection of floral induction pathways using global expression analysis. *Development* **130**, 6001-6012.

Schonrock, N., Exner, V., Probst, A., Gruissem, W. and Hennig, L. (2006). Functional genomic analysis of CAF-1 mutants in Arabidopsis thaliana. *J. Biol. Chem.* **281**, 9560-9568.

Searle, I., He, Y., Turck, F., Vincent, C., Fornara, F., Krober, S., Amasino, R. A. and Coupland, G. (2006). The transcription factor FLC confers a flowering response to vernalization by repressing meristem competence and systemic signaling in Arabidopsis. *Genes Dev.* **20**, 898-912.

Shore, P. and Sharrocks, A. D. (1995). The MADS-box family of transcription factors. *Eur. J. Biochem.* **229**, 1-13.

Simpson, G. G. and Dean, C. (2002). Arabidopsis, the Rosetta stone of flowering time? *Science* **296**, 285-289.

Wang, H., Tang, W., Zhu, C. and Perry, S. E. (2002). A chromatin immunoprecipitation (ChIP) approach to isolate genes regulated by AGL15, a MADS domain protein that preferentially accumulates in embryos. *Plant J.* **32**, 831-843.

Wigge, P. A., Kim, M. C., Jaeger, K. E., Busch, W., Schmid, M., Lohmann, J. U. and Weigel, D. (2005). Integration of spatial and temporal information during floral induction in Arabidopsis. *Science* **309**, 1056-1059.

Wilson, I. W., Kennedy, G. C., Peacock, J. W. and Dennis, E. S. (2005). Microarray analysis reveals vegetative molecular phenotypes of Arabidopsis flowering-time mutants. *Plant Cell Physiol.* **46**, 1190-1201.

Yoo, S. K., Chung, K. S., Kim, J., Lee, J. H., Hong, S. M., Yoo, S. J., Yoo, S. Y., Lee, J. S. and Ahn, J. H. (2005). CONSTANS activates SUPPRESSOR OF OVEREXPRESSION OF CONSTANS 1 through FLOWERING LOCUS T to promote flowering in Arabidopsis. *Plant Physiol.* **139**, 770-778.

Yu, H., Xu, Y., Tan, E. L. and Kumar, P. P. (2002). AGAMOUS-LIKE 24, a dosage-dependent mediator of the flowering signals. *Proc. Natl. Acad. Sci. USA* **99**, 16336-16341.

Yu, H., Ito, T., Wellmer, F. and Meyerowitz, E. M. (2004). Repression of AGAMOUS-LIKE 24 is a crucial step in promoting flower development. *Nat. Genet.* **36**, 157-161.

Zuo, J., Niu, Q. W. and Chua, N. H. (2000). Technical advance: An estrogen receptor-based transactivator XVE mediates highly inducible gene expression in transgenic plants. *Plant J.* **24**, 265-273.